Conference Paper, Published Version

Ghasemi, A.; Mehdinia, M.; Firoozabadi, B.; Afshin, H.

A Comparative Study of the Immscible Density Currents Using the SPH And VOF-LES Methods

Proceedings of ninth International Conference on Hydro-Science and Engineering (ICHE 2010), IIT Madras, Chennai, India.
2 - 5 August 2010

A COMPARATIVE STUDY OF THE IMMSCIBLE DENSITY CURRENTS USING THE SPH AND VOF-LES METHODS

Ghasemi A.[1], Mehdinia M.[2], Firoozabadi B.[3] and Afshin H.[4]

Abstract: *Gravity currents have been studied numerically by many researchers, using the traditional finite volume methods. In this study, two different methods are used to simulate an immiscible two-fluid lock-exchange configuration; first the relatively newer Lagrangian method of SPH and second the FVM method of VOF combined with the LES (VOF-LES method), for higher accuracy. It has been shown that the SPH method, carefully incorporated, can give results with a comparable accuracy to that of VOF-LES method. Considering the run-time of these simulations (which is several folds larger for the VOF-LES), reveals the benefits of the SPH method, with a view towards the current numerical sources available. All simulations have been carried out in 2D configurations. A code is developed for each of the above mentioned methods. For the SPH simulation, an algorithm which is similar to the so-called SPH projection method has been used. This method consist of three steps; the first two steps play the role of prediction, while in the third step a Poisson equation is used to impose incompressibility. It also benefits from ADT search algorithm for efficient search of neighboring particles. For the VOF-LES simulation, the "cubic root of the volume" delta has been used for filtering and the smaller eddies have been modeled using the dynamic Smagorinsky subgrid scale (SGS) model. The Van-Driest damping function has been used for the near wall simulations, although the first grid point lies well under the $y^+=1$ point. The VOF-LES code has been run under the parallel configuration, using the MPI method. Incorporating the mentioned methods, time evolution of the density current structure has been studied. It has been concluded that the SPH method may predict the front position of the density current close to the LES method (which itself is close enough to the empirical data), however it cannot show the details of the interface.*

Keywords: *lock exchange; gravity currents; dynamic large eddy simulation; smooth particle hydrodynamics; projection method.*

1) INTRODUCTION

Gravity currents are categorized as natural flows, which are generated because of a density

[1] M.Sc. Student, School of Mechanical Engineering, Sharif University of Technology, Tehran, Iran
Email: amir_ghasemi@mech.sharif.edu
[2] M.Sc. Student, School of Mechanical Engineering, Sharif University of Technology, Tehran, Iran
Email: mahdinia@mech.sharif.edu
[3] Professor, School of Mechanical Engineering, Sharif University of Technology, Tehran, Iran
Email: firoozabadi@sharif.edu
[4] Assistant Professor, School of Mechanical Engineering, Sharif University of Technology, Tehran, Iran
Email: h_afshin@mech.sharif.edu

difference. This density difference may arise from a non-uniform temperature distribution, chemical constituents or the solid particles suspended in the current. Density currents can be found in the events of discharge of a large amount of particles into a quiescent water reservoir, fall of an avalanche, winds, cyclones or Gulf Stream oceanic current.

The lock exchange flow configuration which is studied in this article is one of the well known cases of the density current flows which have been studied largely both experimentally and numerically. Amongst the experimental studies are the valuable works of Hacker et al. (1996) and Rottman and Simpson (1983). Recently flourishing numerical methods in this area include the LES and DNS techniques. For instance one can refer to the LES simulations of Ooi et al. (2007, 2009) and DNS simulations of Hartel et al. (2000). Despite the high resolution and details that these special FVM methods may provide, they impose large computational costs. Density currents may also contain particles which are named turbidity currents. Simulation of these flows by existing FVM methods would be laborious, but obviously it would be more straightforward to use the particle methods and this motivates one to follow these Lagrangian methods in this area. Currently the SPH method can be considered as the most successful particle approach. SPH was first proposed by Lucy (1977) and separately by Gingold and Monaghan (1977) in astrophysics applications and recently its uses has been grown more in fluid mechanics area. As far as it is known to the authors of this article, the only SPH lock exchange simulation has been performed by Monaghan et al. (1999), who verified his simulation by the experimental results of Rottman and Simpson (1983). It should be mentioned that the main purpose of that paper was another application and the lock exchange flow was used as a test case for it.

In the current study, the case C of Hacker et al. (1996) experiments has been selected and its results support present numerical studies. It should be considered that in both numerical approaches (SPH and VOF/LES) the fluids have been considered as immiscible, while the empirical results pertain to saltwater density currents which can produce some degree of mixing. This inconsistency is due to lack of experimental data in the literature for immiscible lock exchange gravity current.

2) NUMERICAL METHODS

In the following two sections, the numerical approaches of SPH and LES are discussed, respectively. Due to the lack of space, only the main points of formulation are mentioned.

2-1) Smooth Particle Hydrodynamics (SPH)

The SPH scheme used here is a three-step explicit algorithm which is similar to projection method proposed by Cummins and Rudman (1999). This so-called three-step algorithm has been successfully used previously by some researchers (S. M. Hosseini 2007, M. H. Farahani 2008). In the following, a brief review of its three steps is mentioned.

First step: The first steps plays the role of prediction. In this step, body force effect is considered according to Eq. 1, below. It is obvious that in this simulation the gravity force field (g) is the only body force present that acts on the moving particles.

$$\tilde{u}_{t+\Delta t} = u_t + g\Delta t \tag{1}$$

Here u is the velocity and Δt is the time step.

Second step: In the second step, viscous effect is considered. In this article the divergence of the shear stress tensor T_f has been calculated according to a method which first has been proposed by Cleary (1997) and has been successfully used by many authors (Moriss 1997, Shao 2003). This is given by

$$T_f = \sum_b m_b \left(\frac{(\mu_a + \mu_b)\tilde{u}_{ab}}{\rho_a \rho_b \left(\boldsymbol{r}_{ab}^2 + \eta^2\right)} \right) x_{ab}^i . \nabla_a W_{ab} \tag{2}$$

where b shows the neighboring particles, ρ and m are the density and mass of the particles, μ is the dynamic viscosity, $\nabla_a W_{ab}$ is the gradient of the kernel and η is a small number to prevent denominator from becoming zero. $\tilde{u}_{ab}$ and $\tilde{x}_{ab}$ are the difference in velocity and position between particle a and its neighbors b. It should be mentioned that the well-known cubic spline kernel has been used. At the end of the predictin steps the intermediate position and velocity of the particles are calculated as

$$\tilde{\tilde{u}} = \tilde{u} + T_f \Delta t \tag{3}$$

$$\tilde{x}_{t+\Delta t} = x + \tilde{\tilde{u}}\Delta t \tag{4}$$

Third step: Until now no limitation for incompressibility has been considered. In this step the deviation of the particles from incompressibility condition is calculated by continuity equation as

$$(\frac{d\tilde{\rho}}{dt})_a = \rho_a \sum_b \frac{m_b}{\rho_b} \left(\tilde{\tilde{u}}_a - u_b \right) . \nabla_a W(\boldsymbol{r}_a - \boldsymbol{r}_b, h) \tag{5}$$

where h is the smoothing length of the kernel, which throughout this article has been considered equal to 1.3 times the initial distance between the particles. According to Eq. 5, if the particles are moving towards each other, their density in creases and according to the Poisson equation below, their pressure increases and so they repel each other to get closer to satisfy the incompressibility condition.

$$\nabla.(\frac{1}{\tilde{\rho}} \nabla P) = \frac{\rho_0 - \tilde{\rho}}{\rho_0 \Delta t^2} \tag{6}$$

Here ρ_0 and $\tilde{\rho}$ are the initial and deviated densities of the particles, respectively. The SPH form of the Poisson equation according to M. H. Farahani (2008) is as

$$P_a = \left(\frac{\rho_0 - \tilde{\rho}_a}{\rho_0 \Delta t^2} + \sum_b \frac{8m_b}{(\tilde{\rho}_a + \rho_b)^2} \frac{P_b \tilde{x}_{ab} . \nabla_a W_{ab}}{|\boldsymbol{r}_{ab}|^2 + \eta^2} \right) / \beta \left(\sum_b \frac{8m_b}{(\tilde{\rho}_a + \rho_b)^2} \frac{\tilde{x}_{ab} . \nabla_a W_{ab}}{|\boldsymbol{r}_{ab}|^2 + \eta^2} \right) \tag{7}$$

Now by the pressure calculated from previous steps, the Euler equation is used to find the velocity corrections as shown by

$$\widehat{u}_a = -\Delta t \frac{dA}{\tilde{\rho}_a} \sum_b (p_a + p_b) \nabla_a W_{ab} \tag{8}$$

where $dA = dx^2$ is the initial surface of partides. This format of the Euler equation was suggested by Colagrossi (2003), which shows more stable solutions than the more common Euler equation in SPH literatures, which looks like this:

$$\widehat{u}_a = -\Delta t \sum_b m_b \left(\frac{p_a}{\tilde{\rho}_a^2} + \frac{p_b}{\rho_b^2} \right) \nabla_a W_{ab} \tag{9}$$

The final velocity is found by adding the velocity correction to the predicted velocity from steps one and two as

$$u_{t+\Delta t} = \tilde{\tilde{u}}_a + \widehat{u}_a \tag{10}$$

The final position of the particles is calculated using the finite difference scheme as

$$x_{t+\Delta t} = x_t + \frac{\Delta t}{2} (u_t + u_{t+\Delta t}) \tag{11}$$

An ADT search algorithm similar to that proposed by Bonet (1991) has been used for efficient search of the neighboring particles.

2-2) Large Eddy Simulation (LES)

To model the immiscible nature of the flow, a volume of fluid (VOF) method has been used. The governing equations are the continuity and momentum equations which are descretized via the finite volume method. In the VOF method, the interface position is calculated by a linear interpolation. The surface tension value in the continuity equation has been assigned a value of 0.07 m^2/s, which is the value for the pure water. Also the molecular viscosity of water has been assumed for both phases (dense and light). These last two assumptions ignore the impact of the substance change on the mentioned properties, across the domain.

For the turbulence modeling of the flow due to its high Grashof and Reynolds numbers (2.3×10^9 and 11000 respectively), a dynamic Smagorinsky model, originally developed by Lilly (1992) is used. The filtered stress $\tau_{ij} = \overline{u_i u_j} - \overline{u_i u_j}$ (over-bar denotes grid-filtered and caret denotes test-filtered) resulting from the application of the grid filter to the momentum equation can be modeled. The non-isotropic part of the grid and test filtered turbulence stresses are modeled as

$$b_{ij} = \tau_{ij} - \frac{1}{3}\delta_{ij}\tau_{kk} = 2C_s\Delta^2 |\overline{S}| \overline{S}_{ij} \tag{12}$$

$$B_{ij} = T_{ij} - \frac{1}{3}\delta_{ij}T_{kk} = 2C_S\hat{\Delta}^2 |\hat{\overline{S}}| \hat{\overline{S}}_{ij} \tag{13}$$

Where Δ and $\hat{\Delta}$ are the grid and test filter widths and τ_{ij} and T_{ij} are the grid and test filtered stresses, respectively. The dynamic model coefficient, can then be found by applying the least square method (by minimizing the modeling error). The result is given by

$$C_s = 1/2(L_{ij}M_{ij} / M_{kl}M_{kl}) \tag{14}$$

The matrices L_{ij} and M_{ij} are given by

$$L_{ij} = -\widehat{\bar{u}_i \bar{u}_j} + \hat{\bar{u}}_i \hat{\bar{u}}_j \tag{15}$$

$$M_{ij} = \hat{\Delta}^2 |\hat{\bar{S}}| \hat{\bar{S}}_{ij} - \Delta^2 \widehat{|\bar{S}| \bar{S}_{ij}} \tag{16}$$

The use of the Dynamic LES model ensures an acceptable behavior of the current near the wall. The top-hat filter has been used for the grid and test filters and a test filter size of twice the grid filter size is used, which has been shown to give reasonable results previously by Lilly (1992). Also the Van-driest damping function (1982) was used on the filter sizes near the wall.

3) CODE VERIFICATION

In order to verify the developed SPH code, the well-known dam break flow has been simulated and the results validated against experimental data and other numerical methods available in the article by Shao (2003). The geometry of the flow is shown in Fig.1, below.

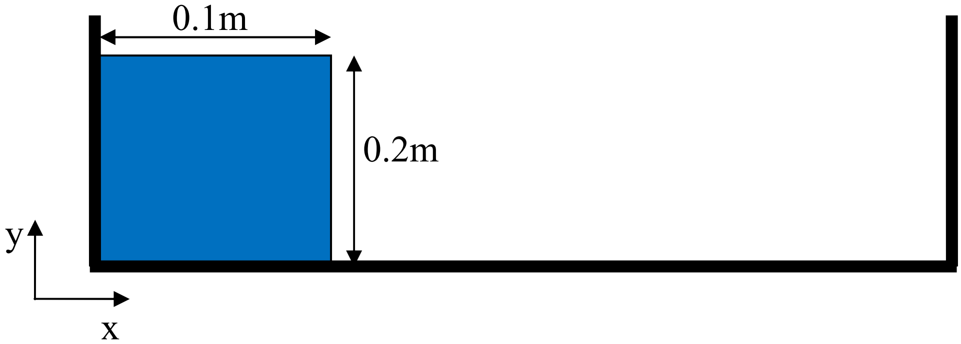

Fig. 1. Schematic geometry of the dam break test case.

The comparison of front position has been shown in Fig. 2. As can be seen, the present code shows good agreement with the experimental and other numerical results. The height of the column of the water (0.2 *m*) is a characteristic length *H* which used to non-dimensionalize the coordinates of the Fig. 2. The total number of the particles used in this simulation is 5000. This simulation verifies the SPH code results.

As for the LES code, due to the lack of space and also the previous articles published by the authors, the code verification results are not presented here. One may refer to the work of Mehdinia et al. (2010) for further information.

4) SOLUTION DOMAIN AND BOUNDARY CONDITIONS

The solution domain pertaining to case C of the Hacker et al. (1996) experiments is shown in Fig. 3. All of the simulations have been performed in 2D configurations. Similar to the Hacker et al.'s experiments the heavy and light fluid densities are taken as 1012 kg/m^3 and 998 kg/m^3, respectively. This results in a corrected gravity $g' = g \times (\rho_{max} - \rho_{min}) / \rho_{min}$ of 12 m/s^2. The lower and Left BCs are taken as walls. The upper boundary has a symmetry boundary condition in LES simulation, while it has been assigned a free surface condition in SPH simulation, which is closer to the experimental setup, having air flow above the domain. The right BC has a convective condition in LES simulation, which uses the algorithm developed by Pierce and Moin (2001). This allows the head to get as close as possible to the outlet.

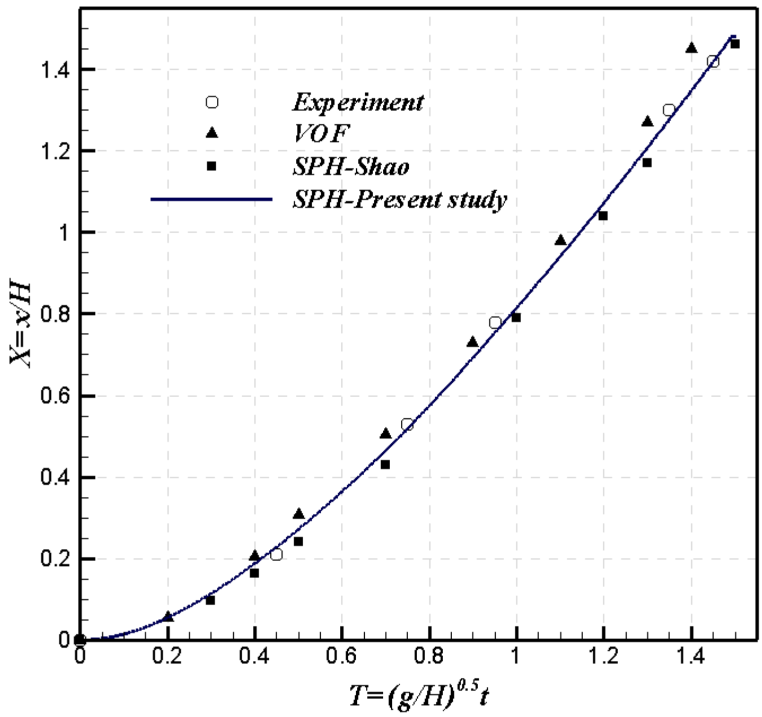

Fig. 2. Comparison of front position of the dam break flow for different studies

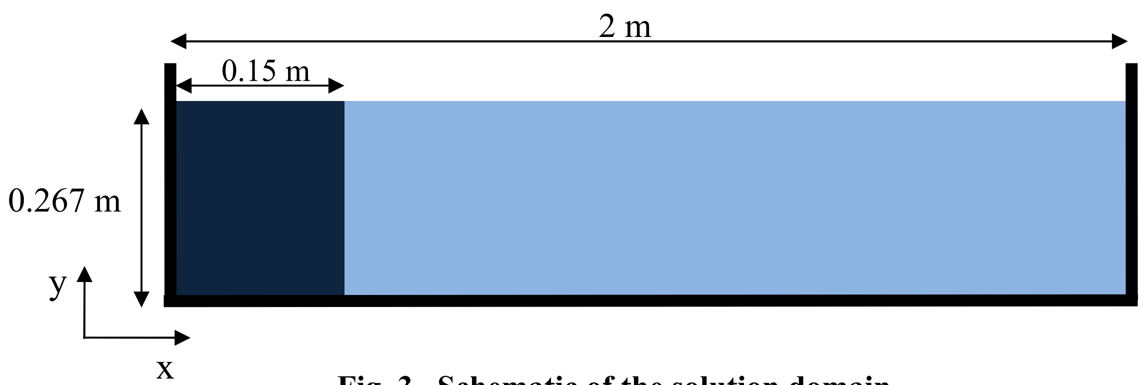

Fig. 3. Schematic of the solution domain

For the SPH simulation, the right BC has been assigned wall condition. Since the simulation results are compared up to 1 *m* of the front lock advance, this imposes no restrictions and the right wall effects may be neglected. For the LES simulation on the other hand, the convective BC lets the head to get as close as possible to the outlet (up to 0.5 *m* distance from the outlet).

5) SOLUTION TECHNIQUES

5-1) Smooth Particle Hydrodynamics (SPH)

For the SPH Simulation, the proposed algorithm is fully explicit and so a small time step size of 0.00002 seconds has been used. This may seem to result in a large computational cost but it should be noticed that since the explicit form of the algorithm solves no system of equations, the amount of the computation for each step is lower than the common SPH projection algorithm. This fine amount of time step size has another advantage that through the steps, the positions of the particles do not vary so much and this means that the neighboring particles also do not change much and it is not needed to search for them every step. Here, every 50 steps one search has been done. Total number of 10800 particles have been used in SPH simulation which resulted from 0.0075 *m* particle initial spacing. To model wall boundary conditions three layers of SPH particles have been considered and the continuity and Poisson equations are solved for them similar to fluid particles, except that the wall particles are fixed. This is done in order to prevent the penetration of fluid particles to the boundary. It should be mentioned that the wall particles only repel the incoming fluid particles and do not attract the particles that are moving away.

Experience with the current algorithm shows that it gives better results for moderate density ratios across the phases. Since the present study simulates the saltwater flow, this density difference is too small. So to overcome the problem, a larger density difference and smaller gravity acceleration have been assumed, in a manner resulting in a corrected gravity of 0.12 m/s^2.

5-2) Large Eddy Simulation (LES)

To descritize the flow equations in the LES simulations, the QUICK algorithm has been used for the divergence and laplacian terms. The Gradient term on the other hand is descritized by a fourth order central scheme as described by Peer et al (2008). The temporal term is also descritized by a second-order backward method. The resulting equations are solved by the preconditioned biconjugate gradient method with the Diagonal incomplete LU asymmetric priconditioner. The iteration process is repeated for each equation until the relative error falls below 10^{-5}. The time step sizes are chosen equal to 0.008 sec, which guarantees the Courant number to be lower than 0.2 and the SGS to dynamic viscosity ratio below 10. A mesh size of 1500×300 has been used for the LES simulations, resulting in y^+ (wall units) less than one in the vicinity of the solid walls.

6) RESULTS AND CONCLUSIONS

LES and SPH contour results are shown in Fig. 4. As can be seen, they show reasonable similarity. However as was expected before, LES demonstrates more details of the flow. It should also be considered that in SPH simulation the number of the particles is about 2.4 percent of the LES mesh number. In contrast to the LES miscible simulation, (which will be presented briefly later), the current immiscible simulation does not clearly show the expected Kelvin-Helmholtz instability at the interface between the fluids. The same fact holds true for the SPH simulation, although SPH inherently is not very successful in Kelvin-Helmholtz instability modeling as discussed by Agertz et al. (2007). Recently, Price (2008) has proposed some remedy for the problem and has deduced considerable improvements for miscible density currents. In Fig. 5, the front position comparison resulting from two numerical approaches and experiments is shown.

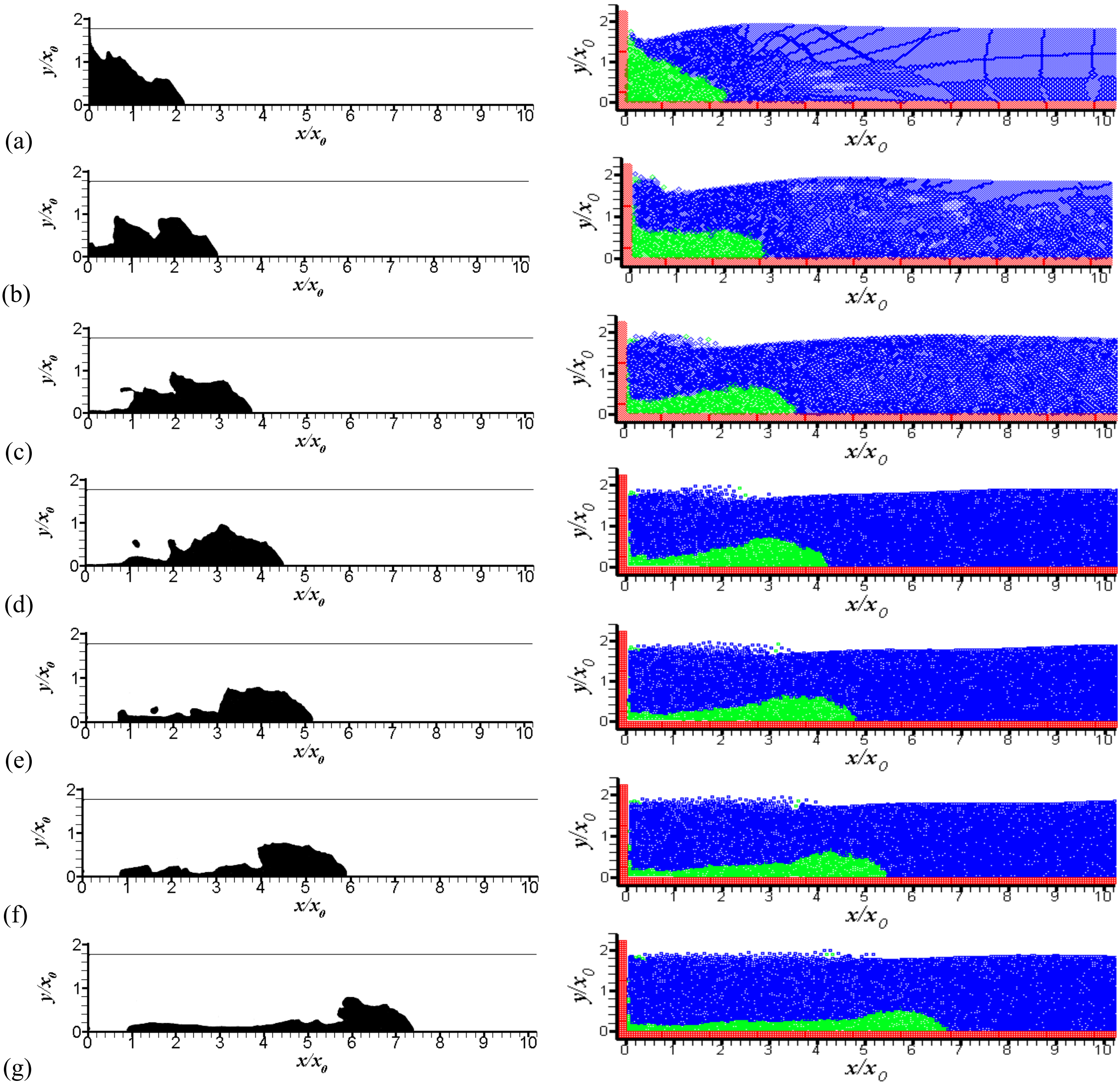

Fig. 4. LES and SPH contour results for (a) t/t_0=1.7; (b) t/t_0=2.7; (c) t/t_0=3.7; (d) t/t_0=4.7; (e) t/t_0=15.6; (f) t/t_0=6.6; (g) t/t_0=8.6; t_0 is defined as $h/\sqrt{g'h}$

As was explained before, the experimental results are generated from miscible saltwater density current but immiscible fluids have been considered for both numerical approaches so the precise matching between numerical and experimental results is not completely expected, although the LES results are more accurate. Maximum difference between LES and SPH front prediction is about 8% which seems reasonable by considering effects of upper free surface and right wall boundary conditions in SPH simulation that are different from the LES approach. The LES method itself may suffer from 2D effects, which causes the front position to fall slightly behind the empirical data. This is shown by Ooi et al. (2002).

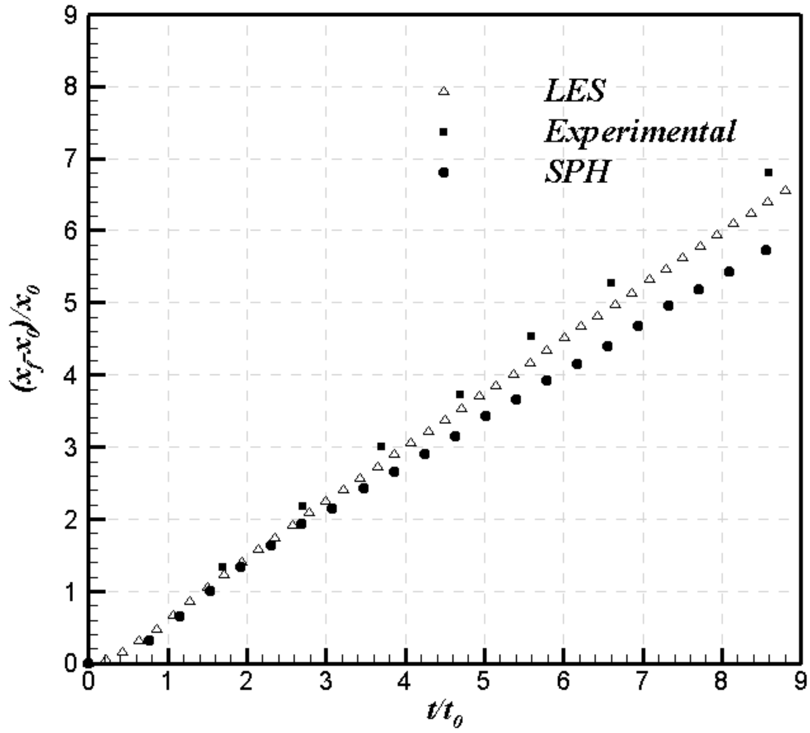

Fig. 5. Front position comparison between LES, Experimental and SPH results.

According to Herbert (1980), the current travel time periods can be categorized into four phases. First, the current accelerates via the heavier fluid spreading over the bottom. After this short phase, the slumping phase ensues, where the current moves with a constant velocity. This can be clearly seen in the linear front position diagrams for three approaches in Fig. 4. The third and the fourth stages known as the inertial and viscous phases respectively ensue at larger times and so they will not be developed here. The goal of this article was to show that the SPH method can predict the front position of the gravity current even by considerably low number of particles relative to LES meshes number, however the current SPH algorithm cannot show the details of the interface.

7) A SIDE STUDY FOR THE LES SIMULATION

An LES simulation for miscible fluids is also performed and it's results for non-dimensional times of 3.7 and 6.6 are presented in Fig. 5. As was stated previously, the Kelvin-Helmholtz instability in the common interface is shown more vividly in contrast to the immiscible LES and SPH simulations. By direct comparison of Fig. 5and Fig. 6 one can see that the front position of the miscible simulation is closer to the experimental data than immiscible one which was expected, before. It should be mentioned that the purpose of this article was a simulation of immiscible density currents.

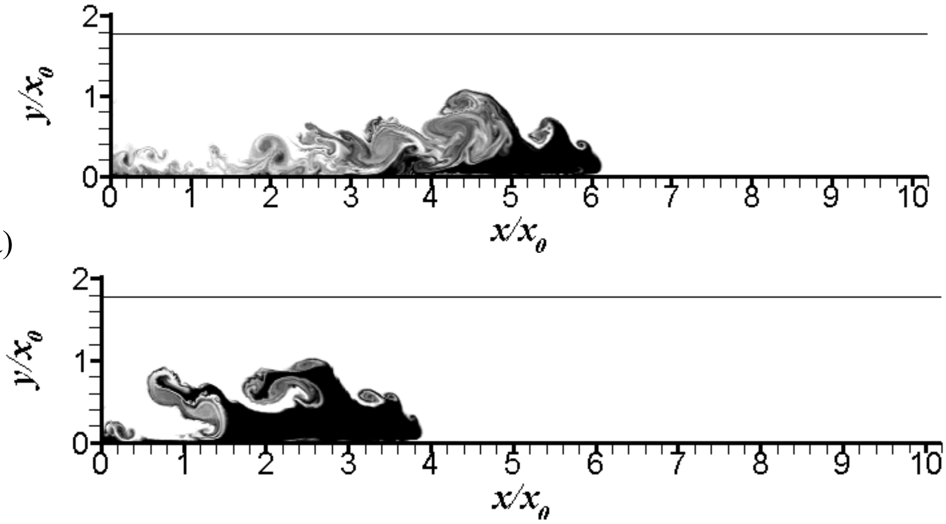

(a)

(b)

Fig. 6. Miscible LES contour results for (a) t/t_0=3.7; (b) t/t_0=6.6

REFRENCES

Agertz, O., Moore, B., Stadel, J., Potter, D., Miniati, F., Read, J., Mayer, L., Gawryszczak, A., Kravtsov, A., Monaghan, J., Nordlund, A., Pearce, F., Quilis, V., Rudd, D., Springel, V., Stone, J., Tasker, E., Teyssier, R., Wadsley, J., Walder, R., 2007. Fundamental differences between SPH and grid methods. *MNRAS,* 380, 963–978.

Baldy, S. 1988. Bubbles in the close vicinity of breaking waves: Statistical characteristics of the generation and dispersion mechanism. *J. Geophysical Research*, 93 (1), 8239-8248.

Colagrossi, A. and Landrini M. 2003. Numerical simulation of interfacial flows by smoothed particle hydrodynamics. *J. Comput. Phys*., 191, 448-475.

Donelan, M.A. 1978. Whitecaps and momentum transfer. *NATO Conf. on Turbulent fluxes through the sea surface, wave dynamics, and prediction,* Ed. A. Favre and K. Hasselmann, Plenum, NY, 273-287.

Farahani, M. H., Amanifard, N., Asadi, H. and Mahnama, M. 2008. Fluid-structure interaction simulation with free surface flows by smoothes particle hydrodynamics. *ASME congress and Exposition, Massachusetts, USA.*

Gran, S. 1992. *A course in ocean engineering*. Elsevier, 583.

Hacker, J., Linden, P. F. and Dalziel, S. B.1996. Mixing in lock-release gravity currents. *J. Dyn. of Atmos. and Oceans*, 24, 183-195.

Hartel C., Meiburg, E. and Necker, F. 2000. Analysis and direct numerical simulation of the flow at a gravity-current head. Part 1. Flow topology and front speed for slip and no-slip boundaries", *J. Fluid Mech.*, 418, 189–212.

Hosseini, S.M. and Amanifard, N. 2007. Presenting a modified SPH algorithm for numerical studies of fluid-structure interaction problems. *IJE Trans B: Applications*, 20, 167-178.

Hwang, P.A., Hsu, Y.H.L. and Wu, J. 1990. Air bubbles produced by breaking wind waves: a laboratory study. *J. Phys. Oceanography*, 20, 19-28.

Lilly, D. K. 1992. A proposed modification of the Germano subgrid-scale closure method. *Phys. of Fluids*, 4, 633-635.

Mehdinia, M., Firoozabadi, B. and Farshchi, M.2010. Large Eddy Simulation of Lock Exchange Gravity Currents. *XVIII international conference on water resources*, Barcelona, Spain.

Moin, P. and Kim, J. 1982. Numerical investigation of turbulent channel flow. *J. Fluid Mech.*, 118, 341-377.

Monaghan, J.J. 2005. Smoothed particle hydrodynamics. *Rep. Prog. Phys.* 68, 1703-1759.

Monaghan, J.J., Cas, R.A.F., Kos, A.M. and Hallworth, M. 1999. Gravity current descending a ramp in a stratified tank. *J. Fluid Mech*. 379, 39-69.

Morris, J.P., Fox, P.J. and Zhu, Y. 1997. Modeling low Reynolds number incompressible flows using SPH. *J. Comput. Phys*. 136, 214-226.

Ooi, S. K., Constantinescu G. and Weber, L. J. 2007. 2D Large-Eddy Simulation of Lock-Exchange Gravity Current Flows at High Grashof Numbers. *J. Hyd. Eng. ASCE*, 133, 1037-1047.

Ooi, S. K., Constantinescu, G. and Weber, L. 2009. Numerical simulations of lock-exchange compositional gravity current. *J. Fluid Mech.*, 635, 361-388.

Peer, A. A. I., Gopaul, A., Dauhoo, M. Z. and Bhuruth, M. 2008. A new fourth-order non-oscillatory central scheme for hyperbolic conservation laws. *App. Num. Mathematics*, 58, 674-688.

Pierce, C. D. and Moin, P. 2001. Progress-variable approach for large eddy simulation of turbulent combustion. *Rep. TF-80, Mech. Eng. Department, Stanford Univ.*

Price, D.J. 2008. Modelling discontinuities and Kelvin-Helmholtz instability in SPH. *J. Comput. Phys*. 22, 10040-10057.

Shao, S.D. and Lo, E.Y.M. 2003. Incompressible SPH method for simulating Newtonian and non Newtonian flows with a free surface. *Advances in Water Resources*, 26, 787-800.